Characterization of Modeling and Experimental Data Inconsistencies from Burst Testing for High-Burnup Commercial Fuel Rod Applications

Nathan Capps[1] and Ryan Sweet[1]
[1]Oak Ridge National Laboratory

ABSTRACT

Fuel fragmentation, relocation, and dispersal are some of the largest issues remaining in the nuclear industry before rod-average burnup can be increased beyond 62 GWd/tU. The issue is primarily related to the potential for fuel to be dispersed into the reactor primary system, which may increase public risk. One way to prevent dispersal is to avoid cladding burst. The objective of this work is to support the high burnup safety case by evaluating cladding burst under high-burnup, full-length fuel rods and to identify uncertainties that could improve model predictions. The results of this analysis will evaluate realistic, prototypic loss-of-coolant accident (LOCA) conditions; support future cladding burst test designs; and inform the development of mechanistic material models. Realistic high-burnup operating conditions were implemented in the BISON fuel performance code to simulate steady-state and LOCA transient fuel rod evolution to the point at which cladding burst occurred. Parametric studies are performed to assess code response to changes in rod internal pressures and heating rates. Results were compared with simulated LOCA experiments to identify inconsistencies between commercial fuel rod analysis and experimental validation. The representative full-length fuel rod LOCA simulation results did not agree with cladding burst tests. Cladding burst tests indicated burst occurring well below (100-150 °C) those calculated in the full-length fuel rod LOCA analysis. Further investigation indicated that the cladding burst tests do not appear to be representative for full-length fuel rods. The inconsistency investigated in this work showed that the differences between the BISON simulation and the experiment's cladding burst conditions arise from an incomplete characterization of the cladding surface temperature, detailed rodlet characterization, lack of cladding strain measurements, and uncertainty in the cladding creep and failure models.

1. Introduction

The United States (US) nuclear industry plans to extend the peak rod-average burnup beyond 62 GWd/tU, which will likely require additional safety analyses beyond what is currently accepted by the US Nuclear Regulatory Commission (NRC). One such analysis might require the nuclear industry to evaluate the fuel evolution during a loss-of-coolant accident (LOCA) to determine the extent of fuel fragmentation, relocation, and dispersal (FFRD), as well as its potential consequences. FFRD was first observed in the Halden Integral Fuel Assessment (IFA) 650 test series [1, 2] in which high burnup (>62 GWd/tU) fuel pellets pulverized into sand-like particles (particles <1 mm), relocated into the balloon region of the cladding, and dispersed through the cladding breach. As a result, the NRC has indicated that the US nuclear industry must sufficiently address the safety concerns stemming from FFRD [3]. One approach could consider evaluating cladding performance to understand whether cladding burst occurs during the LOCA event. Additionally, in the event of a burst, it is important to know at what burst temperature burst occurs and how large the burst opening might be because both conditions could mitigate or potentially exacerbate the extent of FFRD, as well as subsequent consequences. There are other important parameters (e.g., strain) that could be impacted by the burst temperature or directly impact burst temperature and FFRD consequences. This manuscript will assess cladding LOCA performed under prototypic conditions and compare those results to historical burst test. Performance differences will be investigated to better understand uncertainties and inconsistencies. Additionally, improvements to burst testing, data generation and material model develops will be discussed.

[1] This manuscript has been authored by UT-Battelle, LLC under Contract No. DE-AC05-00OR22725 with the US Department of Energy (DOE). The US government retains and the publisher, by accepting the article for publication, acknowledges that the US government retains a nonexclusive, paid-up, irrevocable, worldwide license to publish or reproduce the published form of this manuscript, or allow others to do so, for US Government purposes. DOE will provide public access to these results of federally sponsored research in accordance with the DOE Public Access Plan (http://energy.gov/downloads/doe-public-access-plan).

[1] Corresponding author: cappsna@ornl.gov

Traditionally, LOCA fuel performance analyses have focused on ensuring that coolable geometry [4–7] is maintained for the duration of the LOCA and on maintaining the cladding's post quench ductility (PQD) to prevent cladding failure during the quench process [8, 9]. PQD is determined experimentally by exposing the oxidizing cladding ring samples to steam (<1,204°C) for a period of time before quenching the sample at some temperature <800°C. Ring sample ductility is measured by performing a ring compression test and measuring the accumulation of permanent strain before failure at ~135°C at a predefined displacement rate of 0.033 mm/s [8]. Fuel suppliers and utilities apply this data in conjunction with a series of analyses to ensure that the peak cladding temperature (PCT) of the "hot rod" remains below 1,204°C and the oxide thickness and hydrogen concentration remain below acceptable values [10]. On the other hand, coolable geometry was extensively studied by Erbacher et al. [4–7] through the REBEKA test program [4]. The program consisted of several consecutive test series to evaluate cladding performance spanning from one rod in a steam environment to testing full-length, 7 × 7 assemblies under various flooding conditions. Ultimately, the data generated through the test program were used to develop a heating rate-dependent (°C/s), stress-based burst criteria [5], as shown in Eq. (1):

$$T_R = 3960 - \frac{20.4\sigma}{1+H} - \frac{8{,}510{,}000\sigma}{100(1+H)+2790\sigma}, \quad (1)$$

where T_R is the rupture temperature in degrees Celsius, σ is the engineering hoop stress in kpsi, and H is a ratio of the heating rate defined by Eq. (2) [5]:

$$H = \frac{x}{28}, \quad (2)$$

where x is the heating rate during the LOCA event in degrees Celsius per second.

A secondary objective was to evaluate the flow blockage that resulted from the ballooning and its impact on cooling. Single and full-length fuel rod tests were designed to maximize cladding ballooning in a localized region to quantify the worst-case scenario. The results indicated that 70% flow blockage (indicated to be the maximum) would not impact cooling, and cladding burst would create a secondary quench front that would support additional fuel rod cooling. A final comment made in Erbacher et al. [6] indicated that experimental results showed a greater safety margin than that predicted by licensing tools at that time.

To date, licensed fuel performance codes have historically used spatial simplifications to accommodate the available computing resources. These codes are typically 1D, and in some cases 1.5D, in which the fuel conditions are assessed across a single axial plane or a series of axial planes [11, 36]. Interpolation across a series of axial planes is intended to provide a 2D-like representation across the full length of the fuel rod. Therefore, validating these codes to the experimental data seems very straightforward, provided that the experimental data are radially uniform or can be distilled to 1D. Cladding burst data generally consist of measuring rod internal pressure and local temperature (near the burst region) as a function of time throughout the test until burst occurs; cladding profilometry and burst opening measurements are generally measured after the experiment.

Validating the 1D code against this data seems logical when one considers cladding burst, as indicated by the data, is an inherently nodal failure criterion that requires nodal temperatures and stresses to reach a critical threshold, as defined by Eq. (1). Generally, 1D and 1.5D codes tend to calculate the nodal burst conditions with acceptable accuracy for crucial safety calculations by maintaining a large conservative buffer. However, translating rodlet performance to full-length commercial rods might not be as straightforward and likely leads to more significant conservatisms.

The 1.5D approaches interpolate across axial planes and fail to accurately capture the full effect of the various fuel irradiation processes (e.g., volumetric change, rod internal pressure evolution) associated with LOCA progression. For example, the refill phase consists of injecting water into the core to sufficiently cool the fuel. This process ultimately results in time and axially changing cladding temperature profiles that could result in additional balloons forming prior to burst [16]. This additional

deformation would reduce rod internal pressure and potentially impact subsequent cladding behavior. Secondly, cladding burst tests traditionally impose a cosine-shaped axial heating profile to ensure cladding burst at a specific location. However, the severity of the axial temperature profile tends to be on the order of 50°C over ~5 cm (2 in.) at the expected burst location [12], and 1.5D approaches do not have adequate fidelity to capture these inherently local effects. This severe axial temperature gradient has been observed in the Halden IFA 650.X [1, 2] test series and most recently in the Severe Accident Test Station (SATS) LOCA testing [13], see Fig. 1. Additionally, very little information is known away (~5 cm [>2 in.]) from the burst location, and the temperature presumably continues to decrease, potentially drastically, farther away from the burst location. However, more sophisticated codes, such as BISON, have been able to address the 1.5D model gaps described above.

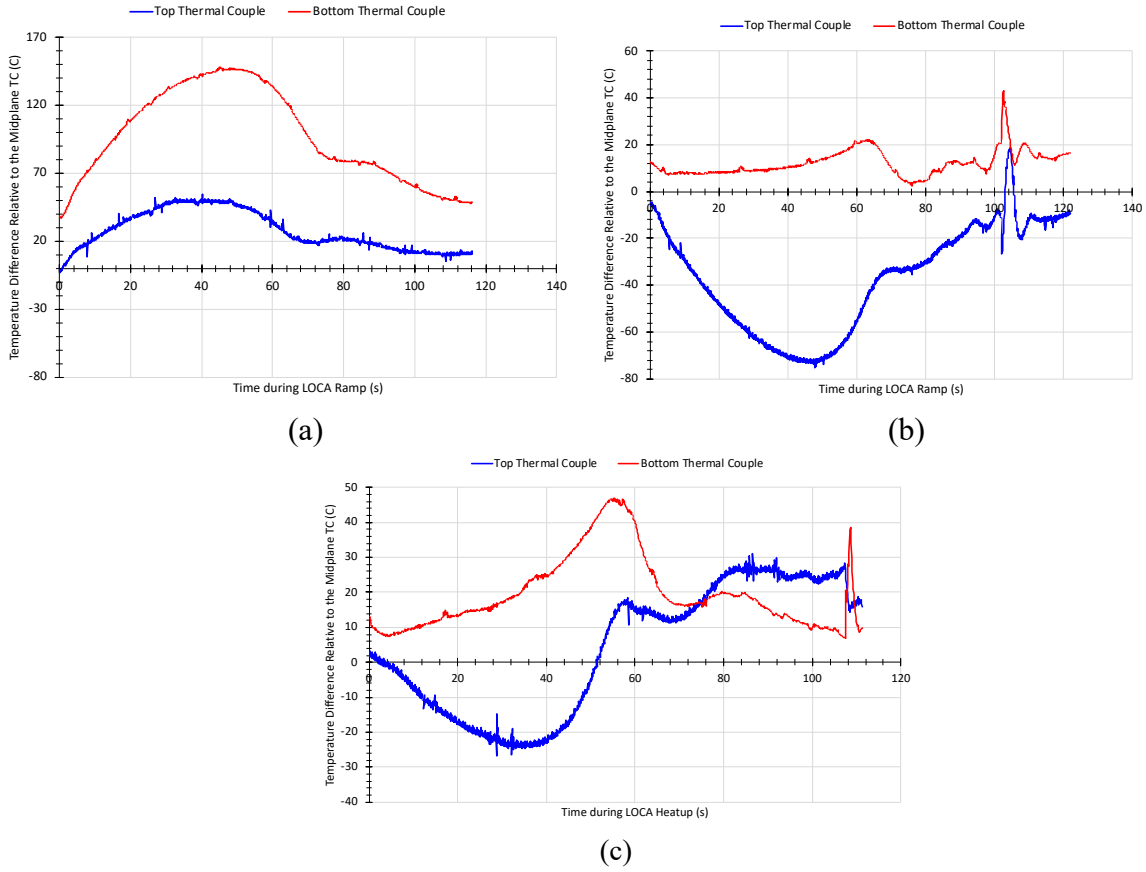

Fig. 1. SATS thermal couple data relative to the midplane thermal couple measurement for a) Zr-20, b) Zr-21, and c) Zr-23

Erbacher et al. [4–7] highlighted the significant impact of an azimuthal temperature gradient on the cladding burst temperature and stresses, and it is reasonable to assume that similar temperature variation will also exist axially along the cladding, although more instrumentation would be needed to measure cladding temperature in more detail. Ultimately, this suggests that current cladding burst models are only valid for 1D analysis and might not be indicative of full-length fuel rod behavior. Furthermore, recent work performed on FeCrAl cladding tubes demonstrated that cladding burst tests could be performed on 10 cm (4 in.) segments instead of 250–300 mm (~12 in.) specimens and generate similar burst conditions (e.g., temperature, balloon geometry, burst opening) as those generated from the traditional 250–300 mm (~12 in.) specimens [14]. Although these tests were not performed on Zircaloy, the results suggest that cladding burst depends on the local effects and not the cladding specimen length. Although the data generated from the burst tests represent nodal (i.e., local) cladding burst conditions, they are not

representative of prototypic LOCA conditions. Prototypic LOCA conditions have a much smaller fuel-to-volume ratio and spatially varying boundary conditions.

This work leverages prior efforts described by Capps et al. [16] to understand cladding performance under high-burnup conditions to prevent fuel dispersal by assessing whether cladding burst occurs. Parametric studies will be performed on known parameters (e.g., heating rate and rod internal pressure) that impact burst timing and cladding strain during the LOCA. These results will be evaluated and compared with experimental data to assess the relationship between cladding burst tests and full-length fuel rod LOCA performance. Additional analyses will be performed to understand the observed differences. The combination of these analyses will be used to inform the development of a prototypic cladding burst test to further validate the full-length fuel rod response. Finally, the results will be used to identify future model development or experimental validation efforts to further improve modeling results.

2. Commercial Fuel Rod Cladding Burst Evaluation Methods

The analyses leverage the BISON fuel performance code [17–21]. BISON has been extensively validated for light-water reactor (LWR) operating conditions, and more specifically, the code's LOCA capabilities were documented in Williamson et al. [21]. The culmination of these validation efforts supports the application of cladding performance and burst evaluation data to commercial fuel rods. Table 1 summarizes the models used in BISON analysis as well as the associated references. Methods used for commercial fuel rod applications will build on previous high-burnup LOCA efforts and will use high-burnup fuel rod operating conditions reported in Capps et al. [16]. The fuel rod operating conditions will remain consistent with those reported in Capps et al. [16] except for the blowdown phase, heating rates, and pre-transient rod internal pressures. These conditions will be modified to develop an operation envelope that encompasses conditions that might be observed during a LOCA event.

Table 1 Summary of the BISON Models and Associated References

Fuel			**Cladding**		
Property	**Model**	**Reference**	**Property**	**Model**	**Reference**
Thermal Conductivity	NFIR	[22,23]	Thermal Conductivity	Fink	[31]
Elastic Properties	MATPRO	[24]	Elastic Properties	MATPRO	[24]
Relocation	Modified ESCORE	[25]	Irradiation Growth	Franklin	[32]
Fission Gas Release	Sifgrs	[26]	Thermal Expansion	MATPRO	[24]
Thermal Expansion	Constant		Thermal Creep	Limback-Anderson and Erbacher	[33,34]
Creep	MATPRO-Halden	[24,27-29]	Irradiation Creep	Hoope	[35]
Solid Swelling	MATPRO	[24]			

The blowdown phase of the LOCA occurs between the rupture of the cold-leg rupture (i.e., $t = 0$ s) and the time at which the primary system pressure decreases to near atmospheric pressures. One attribute of the blowdown phase is the ability for the coolant to continue cooling the fuel while being evacuated through the ruptured cold leg. However, one could conservatively assume that the blowdown phase might not occur, which would result in an immediate increase in cladding temperature. This would ultimately result in additional conservatism because the ECCS would have less time to reduce the cladding temperature. This conservatism would effectively ensure that the PCT remains below 1,204°C but does

not necessarily consider the impact on cladding deformation and burst. Fig. 2 shows an example for each of the two cladding temperature responses: the PCT boundary conditions for a simulation that considers the blowdown and a simulation that does not consider the blowdown. The impact of various pre-transient pressure and heating rates will also be considered under both thermal hydraulic conditions. Table 2 summarizes the simulation matrix used to evaluate cladding performance and burst under high-burnup conditions.

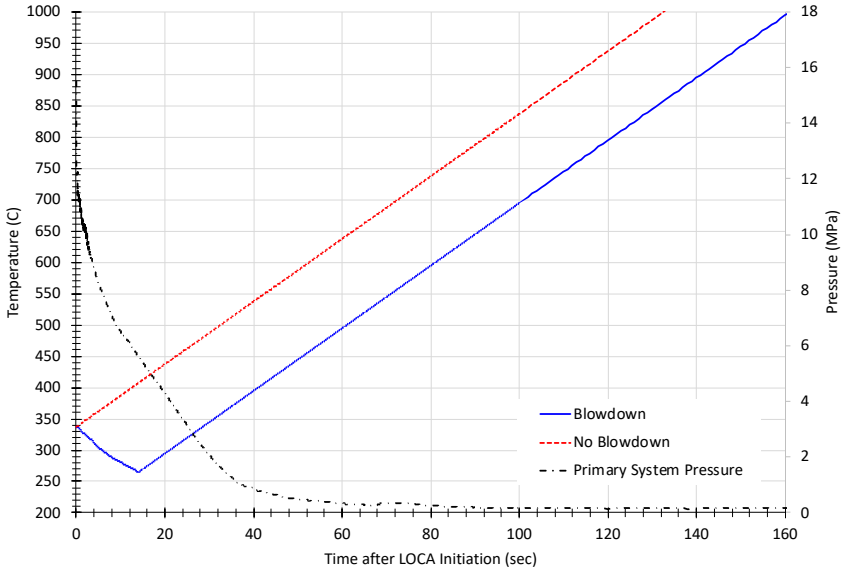

Fig. 2. PCT for the blowdown vs. no blowdown thermal boundary condition at the burst location [16].

Table 2. Full-length fuel rod heating rates and pre-transient pressure conditions [16]

		Pre-transient rod internal pressures at 330°C (MPa) / Pressure differential [RIP-System] (MPa)			
		11.3/-4.2	12.3/-3.2	14.6/-0.9	22.8/+7.3
LOCA heating rates (°C/s)	5	X	X	X	X
	10	X	X	X	X
	15	X	X	X	X
	20	X	X	X	X

Finally, two cladding burst criteria were considered in this evaluation. The first is a stress-based failure criterion used by the NRC in the FRAPTRAN code [11] and described in Eq. (1) [5]. The second is a strain rate–based criterion [36]. Temperatures during a simulated LOCA event are such that Zircaloy rapidly deforms when a rod internal pressure is applied. As temperature increases, the rate of deformation increases until the material is no longer capable of maintaining structural stability, at which time burst occurs. This burst mechanism is attributed to plastic instability and is defined by Eq. (3):

$$\dot{\epsilon} \geq \sim 0.0278\ s^{-1}\ . \tag{3}$$

3. Analysis Results

3.1 Commercial Fuel Rod Analysis

BISON was used to evaluate cladding performance when considering a blowdown and the possibility of cladding heating at the onset of the LOCA (i.e., no blowdown and similar to an infrared furnace burst test). The intent of the analysis is twofold. First, it is necessary to understand whether there are differences between the results. Conceptually, the results are expected to be similar; however, confirmation is required. Secondly, it is important to have a baseline analysis of the fuel rod evolution during LOCAs for both scenarios. Essentially, what does the time evolution look like for key fuel performance parameters, and what impact does this evolution have on fuel performance? The 2-D R-Z results for the two analyses are shown in Fig. 3. Rod internal pressure (Fig. 3a) and temperature (Fig. 3) perform as expected. The blowdown results in the temperature and pressure dropping at constant rates until a quasi-equilibrium is reacted (~20–35 s). This observation is explained by the ideal gas law. As the fuel rod begins to heat, the plenum temperature increases; however, the rod internal pressure continues to decrease rather slowly. One item to note is transient fission gas release (tFGR) is not modeled. TFGR is a phenomenon that occurs under high burnup conditions and occurs as fuel temperature increase to the point where additional FGR beyond that released during steady state irradiation is released. TFGR has the potential to increase the rod internal pressure during a LOCA event and potentially reduce the cladding burst conditions. Currently, BISON does not have a tFGR model specific to LOCA, and there is limited data to accurately develop an empirical correlation. Future work will work to better understand this phenomenon and its impact on cladding burst. This is result of elastic and plastic (i.e., creep) deformation occurring faster than the temperature increase. When removing the blowdown phase, the plenum temperature begins heating immediately; however, the rod internal pressure decreases slightly. This decrease is related to the delta pressure change across the cladding as the system pressure is removed. Removing the system pressure (~15.5 MPa) is enough to cause cladding liftoff and creep, thereby increasing the void volume and decreasing the pressure. Cladding stress and strain are very consistent between the two cases, except for the no blowdown case because it reaches elevated temperatures faster and ballooning occurs sooner (Fig. 3c and 3d).

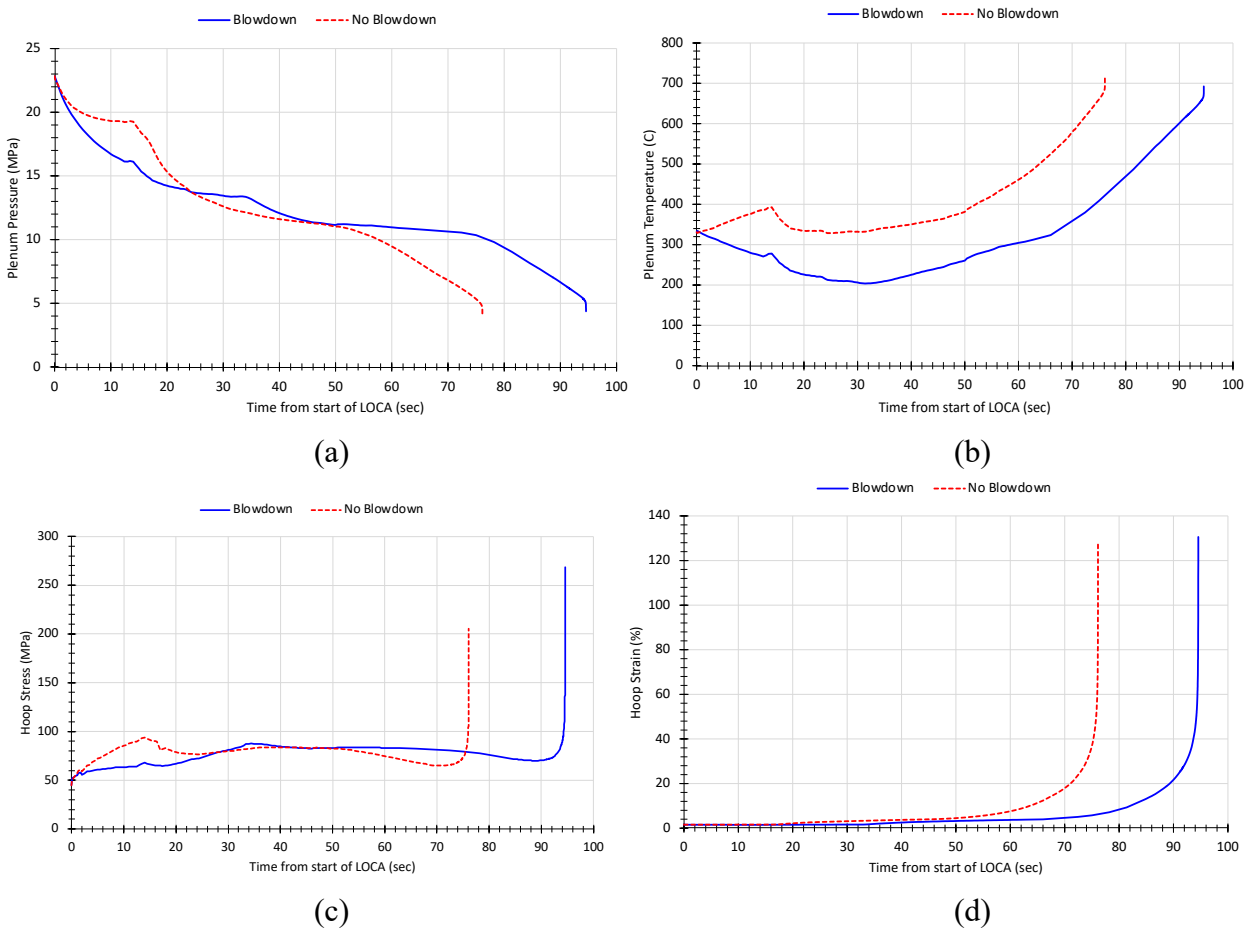

Fig. 3. Analysis assessing the impact of blowdown vs. an event where blowdown is not considered for a heating rate of 5 °C/s and a rod internal pressure of 22.8 MPa.

Table 3 summarizes the burst conditions predicted by the stress and strain rate-based burst criteria. The burst temperature, stress, and peak strain are generally consistent between the two simulations. There is a ~35°C difference in the burst temperature between the stress-based (~747–756°C) and strain rate–based (~780–795°C) failure model. The stress-based failure model provides a more conservative (i.e., lower) burst temperature, whereas the strain rate–based failure model provides a higher burst temperature and a more conservative (i.e., bigger) balloon size. The two results are significant when considering the possible implications on FFRD. For example, bursting at higher temperatures might reduce or possibly mitigate pulverization; however, larger balloon strains—and likely larger burst openings—suggest that the fuel will have a higher propensity to relocate into the ballooned region and ultimately disperse. Bursting at lower temperatures likely increases pulverization susceptibility; however, the balloon strain is smaller and likely has a smaller burst opening; therefore, the fuel will be less likely to relocate and disperse. Both failure models suggest that the cladding will burst at higher temperatures than those observed experimentally. High-burnup and high-pressure (prepressurized to ~11 MPa at 300–330°C) integral LOCA tests performed at Studsvik indicated that burst occurs between 680 and 700°C [37, 38]. However, BISON suggests that a full-length fuel rod with a pre-transient rod internal pressure of 22.3 MPa at ~330°C will not burst until a minimum cladding temperature of ~750°C is reached. This discrepancy between the rodlet burst test and the full-length cladding performance will be evaluated in more detail below.

Table 3. Burst conditions comparison for the blowdown and no blowdown event

	Stress-based burst criteria			Strain rate-based burst criteria		
	Burst Temperature (°C)	Burst Stress (MPa)	Peak Hoop Strain at Burst (%)	Burst Temperature (°C)	Burst Stress (MPa)	Peak Hoop Strain at Burst (%)
Blowdown	747	70	15.2	780	72	27.2
No blowdown	756	65	16.5	795	67	26.3

The previous analysis showed that there are minimal differences between LOCA scenarios that do and do not consider the blowdown phase, provided that the heating rates are identical. This affords an opportunity for a more detailed high-burnup LOCA fuel performance analysis. There are two primary parameters governing cladding performance during the refill phase of a LOCA: (1) pre-transient rod internal pressure and (2) heating rates. Some argue that irradiation-induced embrittlement, hydrogen embrittlement, and oxidation might impact cladding LOCA performance, but there are not enough data to observe any meaningful difference. Furthermore, elevated temperatures will anneal irradiation damage and dissolve hydride precipitates back into solution, thereby countering any potential material degradation. Hydrogen is very important for post-quench ductility; however, this topic is outside the scope of this manuscript. Large oxides could impact cladding performance. However, advanced Zircaloy claddings have shown a drastic reduction in oxide thickness when compared with Zry-4; nonetheless, this will be a topic for future consideration.

Fig. *4* shows an assessment of the impact of heating rate and rod internal pressure on cladding burst temperature (Fig. 4a) and hoop strain (Fig. 4b) using the conservative stress-based burst criteria. Fig. *4*a indicates that the burst temperature increases as the pre-transient pressure decreases and heating rates increase. Again, burst temperatures are noticeably high (>800°C) for such high initial rod internal pressures. Hoop strain results in Fig. 4b are consistent, except for the 22.8 MPa simulations. One possibility is that the high-temperature creep model might be inappropriate for such high rod internal pressure; therefore, balloon strains might be underpredicted. However, increasing the creep rate might increase burst temperatures because the cladding will be more adept at reducing stress. The strain rate-based burst criteria were also considered, and compared with the stress-based failure criteria, the strain rate failure criteria increased cladding burst temperatures by 40°C on average and also increased hoop strains. Both failure criteria show burst occurring at high temperatures; however, the additional burst margin afforded by the strain rate failure criteria could be enough margin to mitigate burst in high-burnup fuel. Additional thermal hydraulic and fuel performance studies that consider possible uncertainties would be needed to confirm.

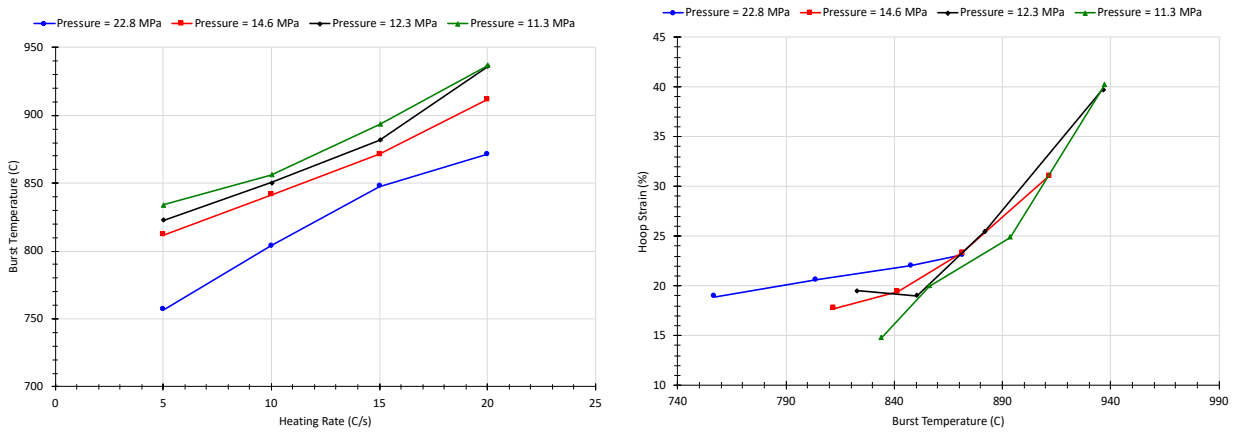

(a) (b)

Fig. 4. Evaluating the impact of (a) burst temperature as a function of heating rate and constant pre-transient rod internal pressure and (b) burst strain as a function of burst temperature and pre-transient rod internal pressure using the more conservative stress-based burst conditions.

3.2 BISON Analysis of Full-Length LOCA REBEKA Experiment

One common difference continues to arise between rodlet burst test and full-length fuel rod burst analyses. The difference is associated with the full-length fuel rod burst temperatures predicted by BISON, which indicate that burst occurs at high cladding temperatures, even with excessively high pre-transient rod internal pressures. What is unclear is why rodlet burst tests differ from full-length fuel rod analysis results. A simple explanation could be that experimental rodlets are ~12× shorter than full-length fuel rods. There are a limited number of LOCA experiments on full-length fuel rods [6, 39], and to date, BISON has been validated against the National Research Universal (NRU) reactor Material Test (MT). BISON validation to some of these fuel rods can be reviewed in Williamson et al. [21]. These tests are important because the pre-test rod internal pressure is ~9–9.5 MPa at ~330°C, which is reasonably close to the results above. The burst conditions were reported to occur at ~805–840°C, and BISON generally predicted the burst temperature accurately for both rods.

The REBEKA test series also performed a simulated LOCA on assemblies that contain full-length fuel rods, and cladding conditions are well characterized for these tests. The optimum case is the REBEKA 2 case in which the fuel rod was heated in a steam environment with burst occurring during the heating phase. Other REBEKA tests have complicated heat transfer conditions, making the analysis very difficult and full of uncertainties in the absence of detailed thermal hydraulic analysis results. REBEKA 2 consisted of a 7 × 7 fuel assembly with nine grid spacers equally spaced across the axial length. Details related to the fuel rod geometries and system conditions are shown in Table 4. One important distinction from other burst tests is that these fuel rods were pressurized at 520°C, whereas many tests pressurize the rods at room temperature or hot zero power conditions (~320°C). Each fuel rod within the assembly contained heating elements that spanned the full length of the tube. A cosine power profile was applied to every fuel rod, and the peak power location was axially located in the center of the fuel rods. The intent was to maximize the local ballooning of each tube to assess the impact of flow blockage on cooling. Fig. ***5*** illustrates the power profile as reproduced from Capps et al. [16]. Cladding temperature measurements were also taken near the burst location and provide BISON with an accurate thermal boundary for performing the validation effort. The measured temperature is shown in Fig. 6.

Table 4. REBEKA 2 fuel rod geometry and test conditions [4, 6].

Test condition	Value	Units
System pressure	0.101	MPa
Heating rate	7	°C/s
Rod internal pressure (at 520°C)	7	MPa
Cladding outer diameter	10.75	mm
Cladding inner diameter	9.3	mm
Cladding thickness	0.725	mm
Segment length	3,900	mm
Cladding type	Zry-4	

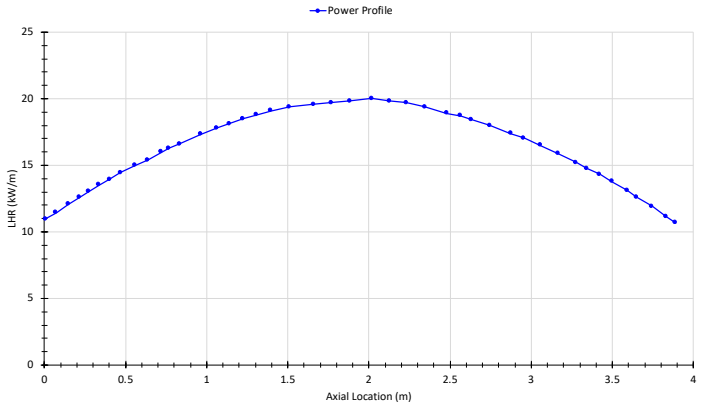

Fig. 5. REBEKA 2 axial power profile [4, 6].

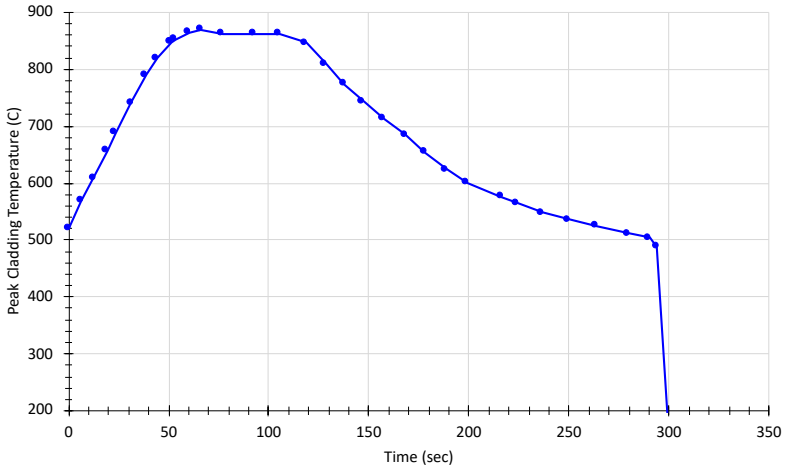

Fig. 6. REBEKA 2 temperature at the burst location [4, 6].

The BISON assessment of the REBEKA 2 fuel bundle LOCA test is shown in Table 5. The stress-based burst criteria under-predicts all experimentally measured conditions. Measured cladding hoop strains ranged from ~20–60% within the fuel assembly with the average shown in Table 5 and Fig. 7. BISON hoop-strain predictions under-predict even the smallest hoop strain value. However, the strain-rate burst criterion predicts near-accurate results, except for hoop strain. The burst temperature was conservative by 2°C, and the burst pressure was slightly lower than measured. The conservative nature of these results is shown in Fig. 7 as the BISON results and failure predictions are compared to the experimental data and stress based burst criteria. Hoop strain results were still lower than the smallest reported strain value.

Excluding hoop strain, BISON burst temperature predictions are conservative, even for a full-length fuel rod. Burst pressure results are considered reasonable, and differences could be the result of subtle differences in the assumed void volume (e.g., plenum length and pellet-cladding gap). Improvements to hoop strain predictions requires in situ 3D stain and stain-rate data to quantify why BISON underpredicts hoop strain. Additionally, there could be azimuthal temperature effects not considered in the analysis that could impact local strain results and are not appropriately reflected in the BISON analysis. However, these subtle changes would not impact the instantaneous rod internal pressure but could impact the burst temperature.

Table 5. BISON comparison to REBEKA 2 experimental result [4, 6]

	Experiment	**Stress-based burst criteria**	**Creep rate burst criteria**	**Units**
Burst Temperature	870	829	868	˚C
Burst Pressure	5.5	5.8	5.2	MPa
Average Hoop Strain	54	6.1	12.5	%

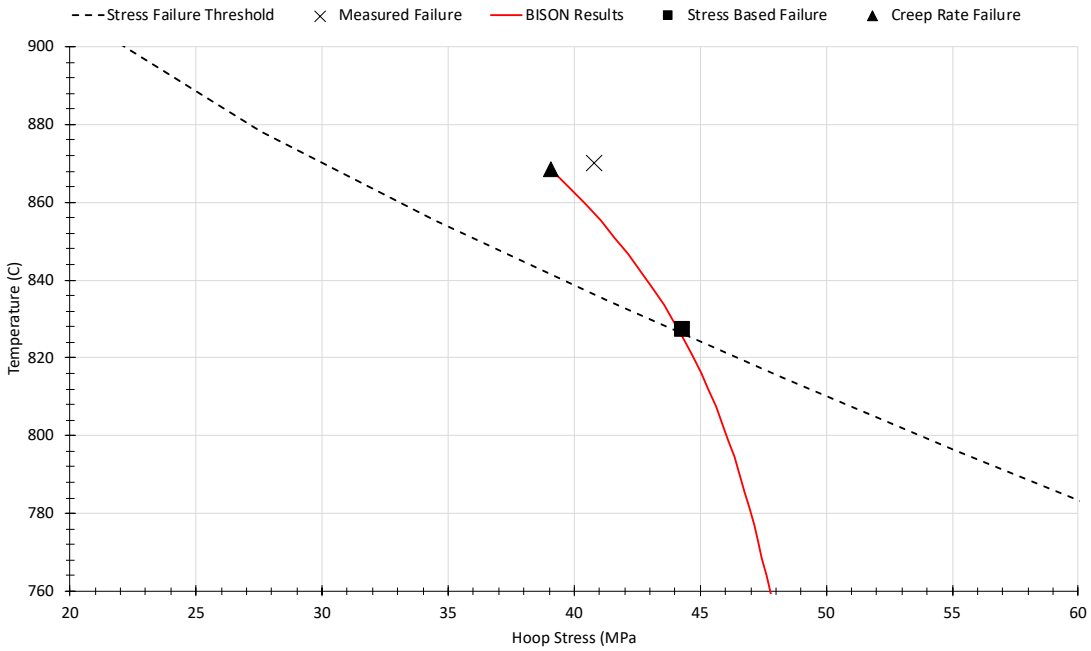

Fig. 7. BISON results compared to the experimental data with a square indicating the stress based failure prediction, a triangle creep rate failure, and X for the experimental data [4, 6].

3.3 Assessing Differences Between the REBEKA Experiment and High Burnup LOCA Simulation

BISON validation against the REBEKA 2 test, as well as results reported in Williamson et al. [21], suggest that the full-length fuel rod analyses are reasonable; however, the validation results do not indicate any of the high-burnup conditions observed in the previous BISON commercial fuel-rod simulations. One consideration might be the peaking factor. The REBEKA and NRU tests had a very pronounced cosine shape, which was intended to maximize the balloon characteristics in a local region. However, peaking factors calculated by RELAP5 suggest that the axial cladding temperature is flatter

than those used in the experiments. This observation is shown in Fig. 8, which compares the time-dependent maximum-peaking factor calculated by RELAP for a high-burnup fuel rod with the REBEKA test maximum-peaking factor. The RELAP-calculated peaking factor remains well below the REBEKA peaking factor for most of the simulation. Eventually, RELAP calculates a higher peaking factor than the REBEKA test because of the quench front pushing the peaking factor toward the upper regions of the fuel rod. Therefore, it is conceivable that the higher burst conditions could be related to the lower peaking factors observed during a "realistic" LOCA.

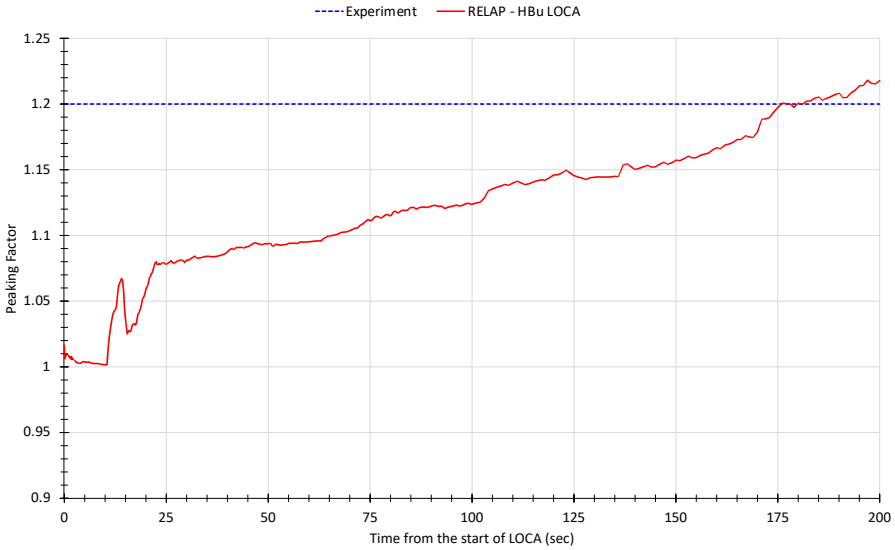

Fig. 8. REBEKA 2 Experimental peaking factor compared with peaking factors calculated by RELAP5-3D for a high-burnup commercial fuel rod [4, 16].

To test this theory, a cladding temperature profile was taken during the LOCA heating phase and applied to the same REBEKA analysis. A comparison between the REBEKA and RELAP axial profiles is shown in Fig. 9. The two axial profiles clearly indicate that the RELAP profile will ensure that the cladding temperature remains flatter over the span of the fuel rod compared with the REBEKA profile. Table 6 summarizes the BISON results between the two simulations. The stress-based and strain-rate failure criteria suggest that the cladding burst temperature increases by 10–15°C while the hoop strain decreases. The change in burst conditions is attributed to the larger void volume generated by the flatter temperature profile, inducing additional axial ballooning. However, the observed difference is minimal when considering the calculated burst conditions are significantly higher than those observed in the rodlet test.

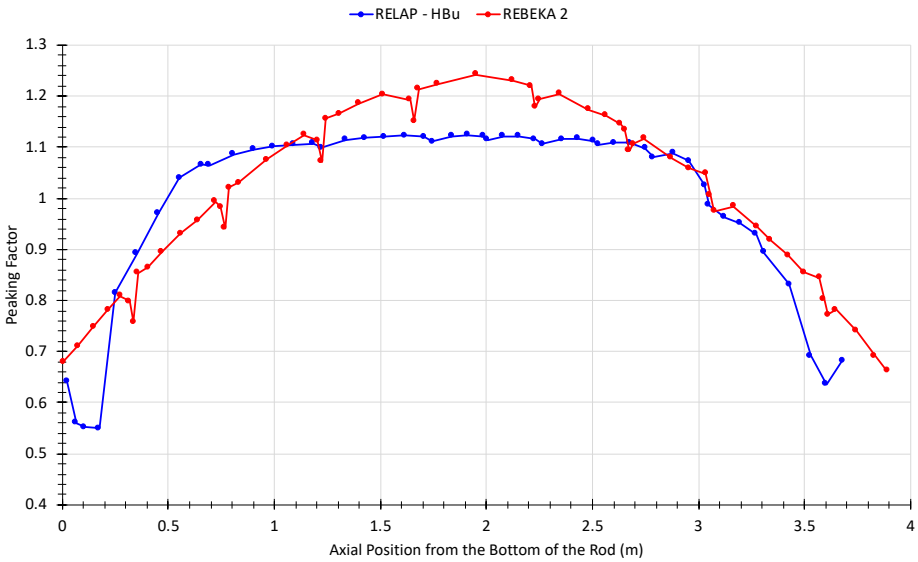

Fig. 9. Comparison between REBEKA 2 and RELAP HBu LOCA axial temperature profiles [4, 16].

Table 6. BISON results evaluating the impact of axial cladding temperature profile on cladding burst conditions [4, 6].

		REBEKA 2 profile		RELAP HBu LOCA profile		
	Experiment	**Stress-based burst criteria**	**Creep rate burst criteria**	**Stress-based burst criteria**	**Creep rate burst criteria**	**Units**
Burst Temperature	870	829	868	844	878	°C
Burst Pressure	5.5	5.8	5.2	5.3	4.6	MPa
Average Hoop Strain	54	6.1	12.5	5.1	9.5	%

One additional scenario not considered in the experiments or axial profile comparison is possible in a commercial reactor LOCA. As indicated in Fig. 9, calculated full-core LOCA cladding temperatures are flatter than what is traditionally observed in an experiment. However, the cladding temperature profile evolves as a function time (Fig. 10). Early in the refill phase, the cladding temperature profile is effectively flat for both the high-burnup (Fig. 10a) and low-burnup hot rod (Fig. 10b) fuel rod. As the quench front progresses, the peaking factor near the bottom of the rod decreases, whereas the peaking factor in the upper region increases. This is consistent with the quench front cooling the bottom regions of the fuel rod while the upper regions remain in a quasi-adiabatic state. Ultimately, this means the instantaneous PCT initially starts at a lower axial location, and as the quench front progresses, the instantaneous PCT progresses upward. This occurrence is shown clearly in Fig. 10b, and the data in Table 7 show that the instantaneous PCT moves ~1 m in the axial direction. Therefore, the cladding at that instant begins ballooning, increasing the void volume and ultimately decreasing the rod internal pressure. However, ~25–50 s later, the instantaneous PCT shifts to a new axial location and starts the ballooning process in the new location higher on the fuel rod. This continues until the PCT comes to rest at a terminal axial location. This process creates a transient ballooning front that results in the initiation of multiple balloons, thereby increasing the void volume and decreasing rod internal pressure so that higher temperatures are required to burst the cladding.

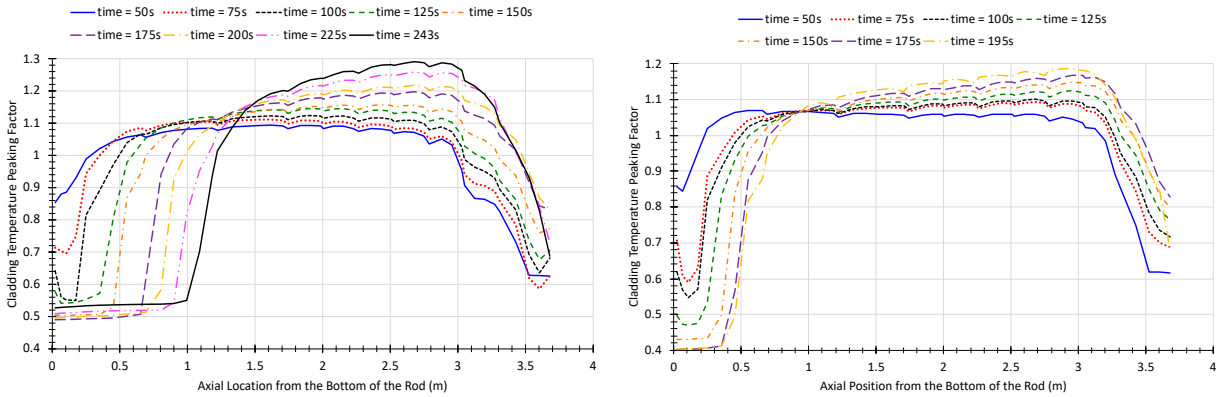

(a) (b)

Fig. 10. Cladding temperature peaking factors as a function of time for (a) high burnup (~72 GWd/tU rod average) and (b) low burnup (~40 GWd/tU rod average) [16].

Table 7. Peak peaking factor for each time and its location

Time (s)	Low burnup		High burnup	
	Location (m)	Peaking factor	Location (m)	Peaking factor
50	0.553	1.070	1.613	1.092
75	2.675 2.955	1.093 1.089	1.613	1.111
100	2.675 2.955	1.100 1.096	1.911	1.123
125	2.675 2.955	1.122 1.124	2.153	1.145
150	2.675 2.955	1.143 1.148	2.433	1.157
175	2.675 2.955	1.159 1.168	2.675	1.197
195	2.601 2.881	1.177 1.187	N/A	N/A
200	N/A	N/A	2.675	1.217
225	N/A	N/A	2.675	1.258
243	N/A	N/A	2.675	1.290

Fig. ***10***b is more complex because the cladding temperature profile remains relatively flat for the duration of the LOCA transient. This is indicative of a hot rod scenario. Like the high-burnup rod, the quench front decreases cladding peaking factors near the bottom; however, the peak peaking factors span across a longer region of the fuel (Table 7). The peak peaking factors shown in Table 7 indicate that the instantaneous PCT occurs in two axial locations separated by a grid spacer or mixing vein. This specific condition allows the cladding to balloon in two different but adjacent axial locations as the grid spacer locally suppresses ballooning mechanically and thermally. The end result is somewhat similar to the high-burnup fuel rod in which the double balloon event increases the void volume and decreases the rod internal pressure. Eventually, a subtle change in the temperature conditions results in the continuation of the ballooning process for one of the balloons, whereas the other balloon comes to rest but not before the burst conditions increase to a point much higher than those observed experimentally.

3.4 SATS Rodlet Evaluation

To demonstrate the difference between the cladding burst model prediction from a cladding rodlet burst test and a full-length fuel rod under LOCA conditions, a burst test simulation was developed for each situation to compare the cladding behavior. During the cladding burst experiment, the cladding is heated

in a furnace by using infrared heaters, and internal pressure is controlled through a pressurized tank with a pressure regulator. The average temperature of the cladding tube is increased to a representative steady-state temperatures and the fill gas is adjusted accordingly. Subsaquently, the cladding temperature is subjected to a standard LOCA temperature ramp until failure occurs.

This test has several challenges when extrapolating to full-length fuel rods. Specifically, the void volume must correspond to the scaled length of the cladding tube specimen, and the temperature gradients must be representative of those experienced in the LWR during the transient. These are important for gas pressure evolution, which is the driving force in the ballooning behavior. With a smaller gas void volume, the internal pressure will decrease more for a given cladding deformation. This allows the cladding balloon to relieve the internal pressure, potentially artificially increasing the temperature that the cladding can withstand. Although sharp temperature gradients, which also directly influence the thermal creep deformation, might not experience the expected increase in gas pressure for a given maximum temperature, this creates a local hot spot in which the cladding is likely to fail, thereby quickly generating smaller balloon lengths.

Burst tests were conducted on Ziraloy-4 cladding tubes via Oak Ridge National Laboratory's (ORNL's) SATS system [13]. Of the tests performed after the initial equipment alignment, one test was selected for benchmarking. This test was selected because of accurate machine calibration and reliability issues with thermocouples in subsequent tests. To approximate the proportion of gas volume in the cladding tube more closely, zirconia pellets were seated in the cladding tube. This test had three stages: (1) the temperature is stabilized during the initial heating, (2) the tube is pressurized and sealed, and (3) the temperature is ramped until the cladding ruptures.

To benchmark BISON against these data, a simulation of this burst test was performed. To construct this simulation, a 2D-RZ representation of this geometry was used along with thermocouple and pressure measurements from the original test, although these data were slightly altered. The thermocouple measurements were used to generate a continuous temperature surface across the cladding to ensure that areas far from the thermocouples still had temperatures prescribed to them. Thermocouples from the original experiment were placed at the cladding midplane and at ± 5.08 cm. from that location. The boundary conditions used here applied to the entire rod length. After the initial gas charge into the cladding tube, the internal pressure was calculated by using the cladding temperature profile and the internal volume similar to that observed in an LWR. This model was modified to account for the additional gas trapped in the line from the gas valve to the cladding, which represents a significant proportion of the gas volume at a lower temperature. The cladding material models used in this analysis are described in a previous analysis [16].

During this simulation, the cladding ruptured at a peak measured temperature of 837 ^{o}C and an engineering hoop stress of 51.6 MPa. Table 8 compares the BISON results with the data from the burst experiment. In the simulation, the cladding bursts at a lower thermocouple temperature and engineering hoop stress. Practically, this is likely an effect of azimuthal temperature variation, which is not captured in the experiment or modeled in this simulation. The variation of the cladding temperature around the cladding circumference is caused by the nonuniform heating conditions in the experiment and leads to hot spots that are likely to cause premature cladding failure [5, 6]. Additionally, because the experiment only measures temperature at three locations along a relatively short span of the cladding, the temperature at the cladding ends is not characterized. This leads to uncertainty in the temperature profile when developing the boundary conditions for the simulation. Lastly, the specific cladding thermal creep model also greatly influences how quickly the cladding will reach failure, and uncertainties here will impact primarily impact the rod internal pressure which impacts cladding behavior during the ballooning phase.

Table 8. Summary of the cladding burst conditions for the experiment and BISON simulation

Data	Peak thermocouple temperature (^{o}C)	Peak engineering hoop stress (MPa)	Peak engineering hoop strain (%)

Zry4-21	837	51.54	37
BISON	788	49.02	12.7

To simulate the LWR LOCA conditions, a nearly flat temperature profile is applied to the previous rodlet test simulation. This corresponds to the conditions from the full-length analysis discussed previously. All other aspects of the simulation are identical; the only change is the temperature gradient. Figure 10 shows the temperature gradients used for these two simulations. Noticeably, the conditions from the actual burst experiment show a monotonically increasing temperature along the axial length of the cladding, and the expected LWR conditions show a gradual cosine shape.

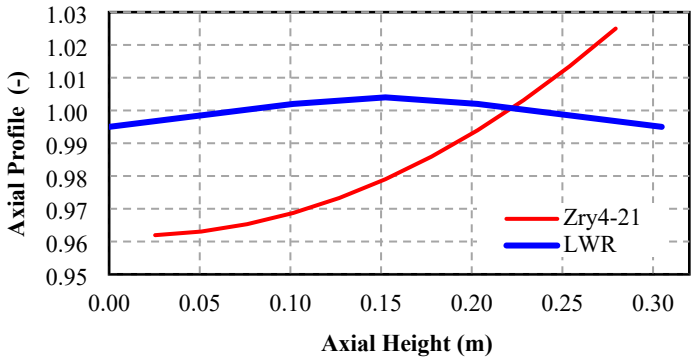

Fig. 11. Axial temperature profiles from Zry4-21 (red) and for the LWR (blue) simulation.

Figure 11 shows the cladding stress vs. maximum cladding temperature for both the cladding burst experiment (Zry4-21) and the corresponding simulation by using the LWR-like temperature gradient. The black dashed line is the stress-based failure criteria for a heating rate of 5°C/s. This figure demonstrates that both cladding simulations burst at higher temperatures when considering the strain rate failure criteria as opposed to the stress-based failure criteria. In general, the LWR simulation reaches an even higher temperature (~30 °C higher).

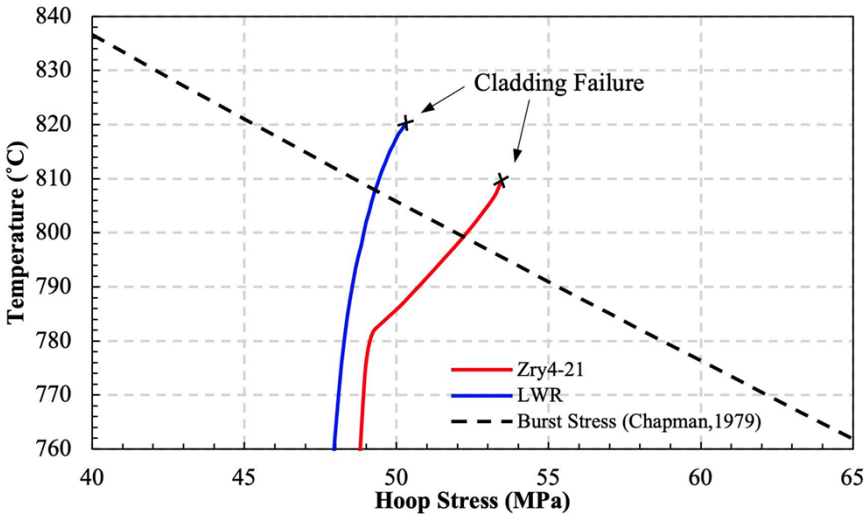

Fig. 12. Cladding rupture temperature and stress for rodlet using measured experiment conditions (red) and LWR-like temperature gradient (blue).

These simulations show that for the more gradual temperature gradient, the cladding deformation is more distributed along the cladding length, which slightly delays rupture relative to the sharp gradient from the burst test. This means that additional consideration might be necessary when applying a failure model

generated in this manner to full-length LWR conditions. Essentially, local variations in the cladding temperature experienced during the experiment can generate models with reduced temperature thresholds.

The ideal burst test will have a more thorough characterization of the cladding temperature, internal void volume, LWR fuel-to-volume ratios, and cladding strain. Although sharp axial and radial temperature gradients can lead to early cladding failure, they are not inherently deleterious effects if the conditions are well characterized. To account for this, additional temperature instrumentation would help better define the cladding temperature surface and capture some of these effects, which can then be modeled. The cladding internal gas volume, including the volume trapped in the test rig gas lines, also needs better characterization. The cladding ballooning process should decrease the internal pressure as it progresses, and as such, the simulation needs an accurate measurement of the total gas volume and temperature to account for pressure drop as the cladding deforms. Finally, the full characterization of the cladding tube strain would allow these simulations to be compared using fully 3D models.

4. Conclusions and Future Work

This paper highlights differences between the expected behavior of commercial fuel rods and cladding experiments under conditions where cladding burst rupture is expected to occur. Evaluations of commercial fuel rod LOCA burst conducted with BISON suggest that commercial fuel rods will burst at higher temperatures than those observed in simulated LOCA tests, and therefore, making historical cladding burst test more conservative. There are several possible reasons for this observed behavior. First, commercial fuel rods are significantly longer (~3.6–3.9 m) than rodlets used in a simulated LOCA test (0.3 m), and because commercial fuel rods have a smaller fuel-to-volume ratio and a changing temperature profile, the rod internal pressure decreases at a faster rate as the cladding deforms. This sustained pressure allows ballooning to occur axially along the cladding with the increased deformation corresponding to higher temperatures. Fuel rod temperatures uniformly increase until the reflood process begins quenching the fuel rod from bottom to top. As the reflood process progresses, local axial regions of the fuel rod cool, thereby terminating the local ballooning process. This results in subsequently smaller changes to the fuel rod's internal volume and pressure conditions. Consequently, upper spans of the cladding tube are subject to increased temperatures for a longer period, allowing larger balloon sizes to form and increasing the likelihood of burst.

However, the results of the representative full-length fuel rod LOCA simulations do not agree with the historical cladding balloon tests. It should be noted that the two scenarios are not equivalent for the reasons stated above, and therefore, these results are not surprising. Cladding burst tests indicated that burst should occur at lower temperatures (<800°C) for similar and even much lower pressures. Looking into the experiments further showed that cladding burst tests were not representative of full-length fuel rod tests and needed to be improved to better represent realistic conditions. The disagreement observed in this work showed differences between the BISON experimental simulations and experiment cladding burst conditions (e.g., stress, strain, temperature) arise from an incomplete characterization of the cladding surface temperature and uncertainty in the cladding creep and failure models. It was determined that improvements to the experiment and to the model were required to adequality represent full-length fuel rod performance.

Future cladding burst tests need more characterization to be more useful for model validation. Typically, the information provided for these tests are the cladding geometry, initial and online pressure, and between one to four thermal couple measurements. Spacial temperature, strain/strain-rate information, or characterization of the void volume are needed for model validation and were demonstrated to affect the experimental results. Incorporating the use of an infrared camera to fully characterize the cladding surface temperature during the burst test would be beneficial. This would enable surface boundary conditions to be collected continuously as the experiment progresses and be implemented into the fuel performance code. Additionally, a high-speed camera could also be used in conjunction with digital image correlation analysis to determine the strain and strain rate of the cladding in-situ. Full cladding surface measurements

provide data used to evaluate and improve thermal creep and failure models, and by monitoring the cladding deformation behavior—along with the temperature—during the experiment, the cladding creep model can be improved and extensively validated. Future cladding burst test should consider incorporating these improvements to minimize data uncertainty and better characterize the test. Additionally, tFGR may impact the rod internal pressure during a LOCA. Future work should consider developing and incorporating an empirical tFGR model based on available data. Axial non-uniformity (i.e., gas communication) should also be considered when incorporating tFGR. Additional tFGR should also be considered to further improve the empirical or mechanistic tFGR model.

Lastly, future work should consider developing a new high-temperature thermal creep and burst model to better capture the impact of microstructural changes on the cladding deformation. The models should be informed by using results from many lower length scale simulations, which are distilled into a simpler form for implementation in the fuel performance code. Enhancing the creep model will enable more accurate simulations of the cladding under rupture conditions and include cumulative effects that may arise from irreversible effects resulting in material degradation and premature rupture. Coupling these model improvements to in situ and high-fidelity cladding creep and burst data will enhance BISON's ability to predict LOCA performance, especially in commercial fuel rod applications.

5. Acknowledgment

The authors would like to thank the Nuclear Energy Advanced Modeling and Simulation program of the US Department of Energy's (DOE's) Office of Nuclear Energy for supporting the fuel analysis. Furthermore, the authors would like to express appreciation to Jason Harp and Caleb Massey of the ORNL Nuclear Energy and Fuel Cycle Division for their support in the review of this manuscript. Lastly, this research used the resources of the High Performance Computing Center at Idaho National Laboratory, which is supported by DOE's Office of Nuclear Energy and the Nuclear Science User Facilities under contract no. DE-AC07-05ID14517.

6. References

1. W. Wiesenack, *Summary of the Halden Reactor Project LOCA Test Series IFA-650*, OECD Halden Reactor Project, HPR-380 (2013).
2. W. Wiesenack, *Summary and Comparison of LOCA Tests with BWR Fuel in the Halden Reactor Project Test Series IFA-650*, OECD Halden Reactor Project, HPR-383 (2015).
3. "Project Plan to Prepare the U.S. Nuclear Regulator Commision for Efficient and Effective Licensing of Accident Tolerant Fuels V1.1", October 2019, https://www.nrc.gov/docs/ML1930/ML19301B166.pdf
4. K. Pettersson et al., *Nuclear Fuel Behaviour in Loss-of-Coolant Accident (LOCA) Conditions*, Nuclear Energy Agency of the OECD (NEA), NEA–6846 (2009).
5. Chapman, R., 1978. Multirod burst test program: progress report. Oak Ridge, Tennessee; Springfield, Virginia, Dept. of Energy, Oak Ridge National Laboratory, US Nuclear Regulatory Commission.
6. F. J. Erbacher, H. J. Neitzel, and K. Wiehr, "Cladding Deformation and Emergency Core Cooling of a Pressurized Water Reactor in a LOCA," Summary Description of the REBEKA Program. Scientific Report KfK 4781, Karlsruhe (1990).
7. D. Powers and R. Meyer, *Cladding Swelling and Rupture Models for LOCA Analysis*, US NRC, Office of Nuclear Regulatory and Research, NUREG-0630 (1990).
8. *ML090900841 – Procedure for Conducting Oxidation and Post-Quench Ductility Test with Zirconium-Based Cladding Alloys*, (2009).
9. M. Billone, Y. Yan, T. Burtseva, and R. Daum, *Cladding Embrittlement During Postulated Loss-of-Coolant Accidents*, NUREG/CR-6967, U.S. NRC, Office of Nuclear Regulatory Research (2008).

10. “Standard Review Plan for the Review of Safety Analysis Reports for Nuclear Power Plants: LWR Edition – Transient and Accident Analysis,” NUREG-0900, Chapter 15.
11. *FRAPTRAN: A Computer Code for the Transient Analysis of Oxide Fuel Rod,* NUREG/CR-6739 Vol. 1, August 2001.
12. Garrison, Ben E., Champlin, Patrick A., Howell, Michael, Cinbiz, Mahmut N., Gussev, Maxim N., Petrie, Christian M., and Linton, Kory D. *Length Dependence of Severe Accident Test Station Integral Testing*. United States: N. p., 2019. Web. doi:10.2172/1566961
13. N. Capps, Y. Yan, A. Raftery, Z. Burns, T. Smith, K. Terrani, K. Yueh, M. Bales, and K. Linton, “Integral LOCA Fragmentation Test on High-Burnup Fuel,” *Nucl. Eng. Des.* 367 (2020) 110811, ISSN 0029-5493.
14. Garrison, Ben, et al. *Length Dependence of Severe Accident Test Station Integral Testing*, United States (2019). Web. doi:10.2172/1566961.
15. H. Zhang, C. Blakely, J. Yu, R. Stewart, and M. Asgari, *Fuel Rod Burst Potential Evaluation under LOCA Conditions for an Existing Plant with Extended Burnup Exceeding the Current Limit by 20%*, INL/EXT-19-55888, September 2019
16. N. Capps, R. Sweet, N. Brown, A. Wysocki, A. Godfrey, B. Collins, S. Lee, N. Szewczyk, and S. Hoxie-Key, “Full Core LOCA Safety for a PWR Containing High Burnup Fuel,” *Nuclear Engineering & Design* (2020), under review.
17. R. L. Williamson, N. A. Capps, W. Liu, Y. R. Rashid, and B. D. Wirth, “Multi-Dimensional Simulations of LWR Fuel Behavior in the BISON Fuel Performance Code,” *JOM* (2016). ISSN 1047–4838.
18. R. Williamson, J. Hales, S. Novascone, M. Tonks, D. Gaston, C. Permann, D. Andrs, and R. Martineau, “Multidimensional Multiphysics Simulation of Nuclear Fuel Behavior,” *J. Nucl. Mater.* 423 (2012) 149–163.
19. R. L. Williamson, K. A. Gamble, D. M. Perez, S. R. Novascone, G. Pastore, R. J. Gardner, J. D. Hales, W. Liu, and A. Mai, “Validating the BISON Fuel Performance Code to Integral LWR Experiments,” *Nucl. Eng. Des.* 301 (2016) 232–244. ISSN 0029-5493.
20. D. Gaston, C. Newman, G. Hansen, D. Lebrun-Grandie, “MOOSE: Parallel Computational Framework for Coupled Systems of Nonlinear Equations,” *Nucl. Eng. Des.* 239 (2009) 1768–1778 209.
21. G. Pastore, R.L. Williamson, R.J. Gardner, S.R. Novascone, J.B. Tompkins, K.A. Gamble, J.D. Hales, "Analysis of fuel rod behavior during loss-of-coolant accidents using the BISON code: Cladding modeling developments and simulation of separate-effects experiments", Journal of Nuclear Materials, Volume 543, 2021, 152537
22. S. YAGNIK, "Thermal conductivity recovery phenomenon in irradiated UO_2 and (U,Gd)O_2", Proc. of Int. Top. Mtg. on LWR Fuel Performance, Parkcity, Utah, 2000.
23. M. LIPPENS and L. MERTENS, "High burnup UO_2 and (U,Gd)O_2 thermal diffusivity measurements and post-irradiation characterizations", EPRI Report TR-106501, 1996.
24. LJ Siefken, EW Coryell, EA Harvego, and JK Hohorst. SCDAP/RELAP5/MOD3.3 Code Manual: MATPRO–ALibrary of Materials Properties for Light-Water-Reactor Accident Analysis. Technical Report NUREG/CR-6150, Vol.4, Rev.2, U.S. Nuclear Regulatory Commission, 2001.
25. Laura P. Swiler, Richard L. Williamson, and Danielle M. Perez, “Calibration of a fuel relocation model in BISON.” In *International Conference on Mathematics and Computational Methods Applied to Nuclear Science & Engineering*, Sun Valley, Idaho, May 5–9 2013. American Nuclear Society.

26. G. Pastore, L. Luzzi, V. Di Marcello, and P. Van Uffelen. Physics-based modelling of fission gas swelling and release in UO_2 applied to integral fuel rod analysis. *Nuclear Engineering and Design*, 256:75–86, 2013.
27. K. Sakai. The fuel creep test IFA-701: results after four irradiation cycles. Technical Report HWR-1039, OECD Halden Reactor Project, 2013.
28. K. Sakai, H. Hanakawa, and T. Tverberg. Investigation of fission induced creep of UO2 and Cr-doped fuel in IFA-701. Technical Report HWR-1006, OECD Halden Reactor Project, 2011.
29. R. Szoke and T. Tverberg. Update on in-pile results from the fuel creep test IFA-701. Technical Report HWR-1092, OECD Halden Reactor Project, 2014
30. G. Pastore, L. Luzzi, V. Di Marcello, and P. Van Uffelen. Physics-based modelling of fission gas swelling and release in UO$_2$ applied to integral fuel rod analysis. *Nuclear Engineering and Design*, 256:75–86, 2013.
31. J. K. Fink and L. Leibowitz. Thermal conductivity of zirconium. *Journal of Nuclear Materials*, 226:44–50, 1995.
32. DG Franklin. Zircaloy-4 cladding deformation during power reactor irradiation. In *Zirconium in the Nuclear Industry*. ASTM International, 1982.
33. M. Limbäck and T. Andersson, "A Model for Analysis of the Effect of Final Annealing on the In- and Out-of-Reactor Creep Behavior of Zircaloy Cladding," in *Zirconium in the Nuclear Industry: Eleventh International Symposium*, ed. E. Bradley and G. Sabol (West Conshohocken, PA: ASTM International, 1996), 448-468
34. F. J. Erbacher, H. J. Neitzel, H. Rosinger, H. Schmidt, and K. Wiehr. Burst criterion of Zircaloy fuel claddings in a loss-of-coolant accident. In *Zirconium in the Nuclear Industry, Fifth Conference, ASTM STP 754, D.G. Franklin Ed.*, 271–283. American Society for Testing and Materials, 1982
35. N. E. Hoppe. Engineering model for zircaloy creep and growth. In *Proceedings of the ANS-ENS International Topical Meeting on LWR Fuel Performance*, 157–172. Avignon, France, April 21-24, 1991.
36. V. Di Marcello, A. Schubert, J. van de Laar, and P. Van Uffelen, "The TRANSURANUS Mechanical Model for Large Strain Analysis," *Nuclear Engineering and Design*, 276 (2014) 19–29.
37. P. A. C. Raynaud, *Fuel Fragmentation, Relocation, and Dispersal During Loss-of-Coolant Accidents*, US NRC, Office of Nuclear Regulatory and Research, NUREG-2121 (2012).
38. M. Flanagan, P. Askeljung, and A. Purana, *Post-Test Examination Results from Integral High Burnup Fueled LOCA Test at Studsvik Nuclear Laboratory*, US NRC, Office of Nuclear Regulatory and Research, NUREG-2160 (2013).
39. J. H. Haberman, LOCA Simulation in the National Research Universal Reactor Program Post irradiation Examination Results for the Third Materials Experiment (MT-3) – Second Campaign. United States (1985). Web. doi:10.2172/1086289.